

Metastability of Cortical BOLD Signals in Maturation and Senescence

Shruti Naik¹, Oota Subbareddy^{1,2}, Dr. Arpan Banerjee³, Dr. Dipanjan Roy⁴, Dr. Raju S. Bapi^{1,5}

¹International Institute of Information Technology (IIIT), Hyderabad

²Teradata India Pvt. Ltd., Hyderabad

³National Brain Research Centre, Manesar

⁴Centre of Behavioral and Cognitive Sciences, Allahabad

⁵School of Computer and Information Sciences, University of Hyderabad, India

Abstract— We assess change in metastability to characterize age-effects on the dynamic repertoire of the functional networks at rest. Resting state fMRI signals from each subject (N=48) have been used and metastability is evaluated as the standard deviation of mean phase synchrony of BOLD signals across whole-brain as well as across known resting state networks. The results suggest that significant whole-brain metastability changes occur between middle to old age. We also demonstrate that static time-averaged FC largely undermines age-effects on the interaction between functional networks. Discriminant Function Analysis reveals existence of two different patterns of change in metastability, which maximally discriminates between two different processes of maturation and ageing.

Keywords—functional MRI; Synchronization; Healthy Ageing; Metastability, connectome

I. INTRODUCTION

Intrinsic activity of the brain in the absence of any task demonstrates spontaneous fluctuation of the spatially distributed networks comprising synchronized regions [1] and at cortical level spatiotemporal patterns of these networks can be captured using functional MRI [2]. Using seed-based and whole-brain graph theoretical measures, studies have revealed age-related changes in these resting state-connectivity patterns [3-5]. These studies often report reorganization of functional networks and changed network properties across lifespan. Overall, long-range functional connectivity (FC) declines with age. However, connectivity within and between functional networks have shown more complex patterns of U or inverted U-shaped curve across lifespan [6]. Graph theoretical analyses of the networks of healthy subjects show that while local efficiency of functional networks declines across lifespan, global efficiency is maintained till the later age [7]. These network changes co-occur with the reduced task-specificity of functional networks during positive task performance [8], which might suggest flexibility of functional networks on top of declining structure [9-11].

Most of these studies use static functional connectivity measures, the grand mean-FC averaged over time. However, recent evidences propose that functional organization of the brain at rest has rich dynamic repertoire, fluctuating between

various possible states in time [12]. The change in dynamic-FC with age predicts brain maturity with good accuracy [13]. Flexibility of d-FC known as ‘metastability’ ; also correlate with flexible cognitive function [14].

Since elderly adults show change of behavioral strategies [15] and also altered spatiotemporal FC patterns, we hypothesize that: 1) metastability of resting state FC will vary significantly across age-groups. & 2) age-effect on metastability would manifest differently across different resting state networks. We adapt an exploratory analysis approach.

First, using signal processing techniques on BOLD time-series data, we improve temporal resolution of the imaging data and define metastability. Secondly, using graph theoretic approach, we detect communities that are consistent across age-groups. We investigate the significance of the first hypothesis of different metastability across age-groups in detected communities and in whole-brain. Furthermore, we divide brain regions in seven pre-defined functional networks namely: Control, Default Mode Network (DMN), Dorsal Attention Network (DAN), Ventral Attention Network (VAN or salience network), Limbic System, Sensorimotor (SMN) and Visual Networks. We first assess age-effects on each of these individual networks. Finally, to test the second hypothesis of changed roles of resting state systems, we carry out discriminant function analysis (DFA) which explores linear combinations of these seven resting-state networks which contributes maximally in discriminating between healthy young, middle-aged and old subjects.

II. MATERIALS AND METHODS

A. Participants

BOLD signal time-series data were obtained for 48 healthy participants (age: 18-80; mean: 41.55 years; 19 males) at the Berlin Centre for Advanced Imaging, Charité University, Berlin, Germany¹. All participants gave written informed consent and the study was performed under compliance of laws and guidelines approved by the ethics committee of Charité University, Berlin. Participants did not show any sign of age-related neurodegenerative diseases under clinical testing procedures at the time of imaging. For the purpose of

¹ DR would like to acknowledge department of Neurology, Charité, Charitéplatz, Berlin for making the data available for this study and for his affiliation with the institute as postdoctoral research associate at the time of data acquisition.

group level analysis in this study, subjects were further uniformly divided as follows: 16 healthy young adults (age: 18-27; mean: 23.25 years), 16 healthy middle-aged adults (age: 28-51; mean: 38.11 years) and 16 healthy old adults (age: 54-80; mean: 65.2 years).

B. Imaging Protocol and Functional Connectomes

Functional MRI and T1-weighted scans (along with other sequences which are not pertinent to the current analysis) were acquired using 3T Siemens scanner. BOLD time-series were acquired at TR 1940 ms lasting 22 minutes (TE 30 ms, FA 78°, 32 transversal slices (3 mm), voxel size 3 x 3 x 3 mm, FoV 192 mm). The Virtual Brain pipeline was used for the preprocessing of the data. Further details regarding the preprocessing steps and image acquisition parameters can be found in [16]. Each participant's functional images were registered to pre-processed T1-anatomical images and parcellated into 68 regions of interest (ROIs) using FREESURFER's Desikan-Killiany atlas [17]. Regional time-series were obtained by considering weighted average from voxel-wise time-series. Subject-specific functional connectivity (FC) matrices were obtained by applying z-transformed pairwise Pearson correlation between each pairs of regional BOLD time-series as well as using phase-synchrony between each pairs of filtered analytic BOLD signals (see *Synchrony and Metastability* section for details) [18].

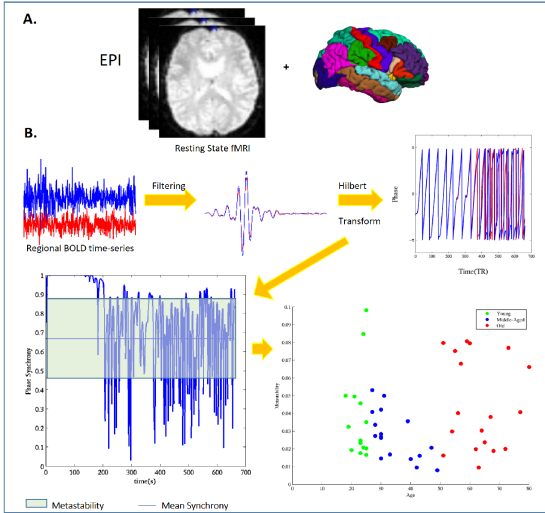


Fig. 1. Illustration of the pipeline followed to characterize metastability. A. Preprocessed data is parcellated and regional BOLD signal is extracted. B. Hilbert transform is applied to filtered BOLD signals to find phase synchrony and metastability.

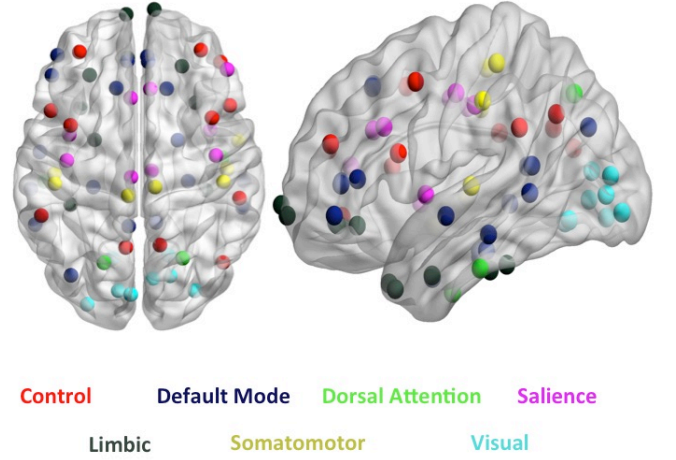


Fig. 2. Centers of the regions categorized in seven resting state networks identified in Yeo *et al* and adapted for the Desikan-Killiany atlas used for this study.

C. Synchrony and Metastability

Each subject's regional BOLD time-series signals were first band-pass filtered in narrow frequency-band 0.04-0.07Hz using Parks-McClellan optimal equiripple filter [18]. Analytic signal (y_n) was derived from each band-pass filtered original BOLD signal as follows:

$$y_n(t) = x_n(t) + j\mathcal{H}(x_n(t)) = Re^{i\phi_n(t)} \quad (2)$$

Where, $\mathcal{H}(x_n(t))$ represents Hilbert transform of the original signal $x_n(t)$ for n^{th} ROI. Analytic signal has advantage over original signal since it discards negative frequency components without loss of information and makes instantaneous phase ($\phi(t)$) of the signal accessible; hence allowing to explore relationships at higher temporal resolution. For each subject, at each time-point, the Kuramoto Order Parameter (R) then defines mean phase synchronization or instantaneous coherence in the network [19]:

$$R_c(t) = \frac{1}{N_c} \left| \sum_{j=1}^{N_c} e^{i\phi_j(t)} \right| \quad (3)$$

Here, N_c represents the number of regions in the network c . For whole-brain analysis, $N_c=68$; for the functional network analysis, N_c depends on the number of regions considered for that particular functional network. Metastability (ξ_c) for each subject is then defined as the amount of variability of brain-wide or community-wide coherence i.e., standard deviation of the Kuramoto Order Parameter.

$$\xi_c = \frac{1}{t-1} \sum_{t=1}^T (R_c(t) - \langle R_c(t) \rangle)^2 \quad (4)$$

We use this measure of metastability to compare across age groups as well as across lifespan. Furthermore, subject

specific functional connectivity matrices were obtained based on the instantaneous phase of the signal such that each entry FC_{ij} in the phase-based matrix FC represents cosine of instantaneous phase-difference between regions i and j ($\phi_i(t) - \phi_j(t)$) averaged over time [20]. These matrices were used for community detection across subjects.

D. Community Detection & Hub Identification

Brain Connectivity Toolbox [21] was used to investigate the modular organization of each participant's FC networks. Modularity quality (Q) was determined by comparing the observed within-module connection density to the expected within-module connection density as follows:

$$Q = \frac{1}{2m} \sum_{ij} [a_{ij} - p_{ij}] \delta(\sigma_i - \sigma_j) \quad (1)$$

Where, $2m$ is total weights of all connections in the network, a_{ij} and p_{ij} are respectively actual and expected weights of connections between nodes i and j . $\delta(\blacksquare)$ is Kronecker delta function, whose value is one, when nodes i and j are in the same community and zero otherwise. Here we used the variant of quality function adapted for accommodating negative edge weights [22]. Optimal community structure was obtained by maximizing Q-value for each partition according to the Newman's algorithm [23].

The modularity algorithm was run for 1000 iterations for each participant's FC. An optimal representative partition was determined with an iterative consensus-clustering algorithm, based on similarities in the 1000 near-optimal community partitions. Depending on the partition, hub regions were determined as the regions whose participation coefficient was greater than mean plus first standard deviation of all participation coefficient values for the subject's community partition. Most consistent hubs across all subjects were then used as seeds to determine the communities, which were common across all subjects.

Same procedure was repeated for the FCs obtained based on Pearson Correlation and phase-synchrony. As shown in Fig. 2 (bottom panel), number of communities detected was similar regardless of the method used for obtaining FC matrix. However, the phase-based FC determined fairly consistent communities across subjects.

Apart from the communities obtained from the above procedure, we also subdivided each region of the brain in seven overlapping functionally important networks previously identified by Yeo *et al* [24](Fig. 2). Taking overlapping networks into consideration allow us to perform exploratory analysis to determine role of each of these networks in classification of healthy young, mid-age and old subjects.

E. Statistical Analysis

For group level analysis, non-parametric one-way analysis of variance was performed using Kruskal-Wallis rank-test [25]. Post-hoc multiple comparison tests were performed if required [26]. To understand combined contribution of

metastability scores of each of the seven resting state networks, we adapted Discriminant Function Analysis [27].

III. RESULTS

A. Most consistently detected communities across subjects.

Fig.3 (top panel) shows communities detected on the mean FC matrices obtained from two different procedures: correlation based (top left) and phase-based (top right). Number of communities varied between three to seven communities per subject. No significant difference was observed between standardized Q-scores obtained on community detection from both the FCs ($t=10^{-4}$, $p=0.5$, paired t-test), which suggests that quality of partitioning was not compromised while using phase-based FC.

Set of hub regions for each individual network was determined by selecting the regions having participation coefficient greater than mean plus first standard deviation of the distribution. Hub list of the most participants included left precuneus, bilateral rostral middle-frontal, right superior parietal cortex, caudal anterior cingulate gyrus, precentral cortex and entorhinal cortex. To determine most consistent partitions across subjects, each of these hub regions were considered as seed and consistency of regions falling in the same community as of seed was determined across subjects. Highest number of participants ($N=34$) had 3 partitions in common: 1. Community1- Default mode/limbic system identified by bilateral precuneus, inferior temporal, inferior parietal, rostral anterior cingulate and isthmus cingulate cortex as well as part of inferior frontal regions.

2. Community2- Control/attention network identified by bilateral frontal-orbital regions, caudal anterior cingulate, insula and supramarginal cortex.

3. Community3- Sensorimotor network involving bilateral precentral, postcentral, paracentral gyrus, superior parietal lobule, cuneus, lingual gyrus and regions from primary occipital cortex.

B. Metastability of elderly adults is significantly higher than that of middle-aged adults.

Kruskal-Wallis rank test was used for comparing median ranks across young, middle-aged and old group. The one-way ANOVA test confirmed that there was statistically significant difference between metastability of young, middle-aged and elderly groups ($H(2)=6.55$, $p=0.038$) with a mean rank of 25.31 for young, 18.68 for mid-age and 31.41 for old group. A post-hoc Scheffe's test showed that metastability of elderly adults differed significantly from that of the middle-aged subjects at $p=0.038$. No significant differences were observed between mean ranks of the other two pairs of groups. Fig. 4 summarizes the group-wise statistics in box-plot.

Similar analysis was performed for the three communities obtained as discussed in above section. Mean values of metastability followed a U-shaped trend across age groups, with middle-aged subjects demonstrating the lowest

metastability in all the communities. However, not all of these results were significant. Fig. 3 (bottom panel) shows mean measures of metastability (\pm standard error) across all communities. Metastability of elderly adults in control/attention network ($H(2)=10.67$, $p=0.0048$) was significantly different than that of middle-aged subjects. No significant age-effects were observed in the metastability of other communities.

C. Metastability of known functional network shows statistically significant differences across age-groups.

As shown in previous analysis, metastability of middle-aged and old age groups across detected communities was significantly different. To gain understanding of functional importance of metastable regions involved in these communities, we further assigned each region to one or more resting state functional networks following the procedure from [28]. Metastability of each functional network for each subject was calculated as the standard deviation of temporal coherence of regions involved in these networks as explained previously. First, nonparametric univariate Kruskal-Wallis tests were performed for test of equality of group means on each of these networks. Results are summarized in table 1 & 2.

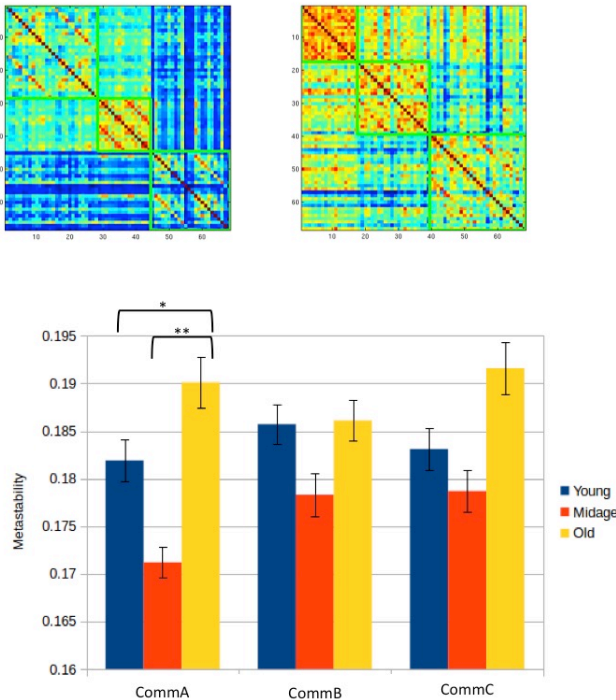


Fig. 3. Communities detected by correlation-FC (top-left) and phase-based FC (top-right) and metastability of the most consistent communities across subjects (bottom). CommA: control + ventral attention regions (identified hub: Insula); CommB: Default Mode/limbic regions (identified hub: Precuneus); CommC: Sensorimotor regions (identified hub: Precentral gyrus)., ** $p<0.005$, * $p<0.05$, Kruskal-Wallis test of mean ranks).

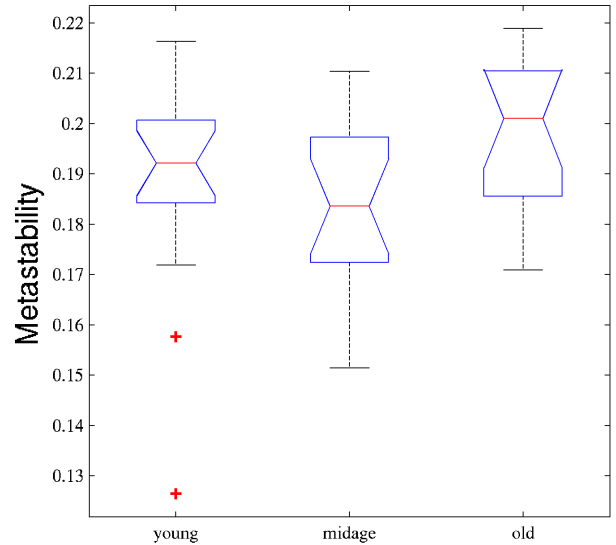


Fig. 4. Box-plot for whole-brain metastability at rest for three age-groups. Horizontal lines represent mean ranks, notches represent 95% confidence interval. Mean rank of middle-aged group is significantly less than that of old group ($p=0.038$).

Significant age-effects were observed in control network, dorsal and ventral attention networks and limbic system ($p<0.05$). Post-hoc analysis revealed significant difference in mean ranks of metastability of younger and middle-aged group for the control network and ventral attention network. Mean ranks of middle-aged and older group were significantly different in dorsal attention network and limbic system. Mean ranks of DMN, SMN and Visual networks for any group-pairs were not significant.

TABLE I. UNIVARIATE TESTS OF EQUALITY OF GROUP MEANS

	Chi-sq	sig	young	midage	old
Control	6.43	.040*	30.94	18.44	26.03
DMN	3.74	.154	21.94	22.56	30.66
DAN	10.72	.004*	25.81	16.74	32.97
VAN	11.85	.003*	29.50	15.38	30.72
Limbic	7.94	.018*	21.75	20.32	33.22
SMN	4.35	.114	24.88	20.03	30.41
Visual	4.53	.104	19.88	24.56	30.59

TABLE II. POST-HOC MULTIPLE COMPARISONS

	Post-hoc	sig
Control	Young-midage	0.032
DMN	NA	-
DAN	midage-old	0.032
VAN	young-midage	0.0127
	midage-old	0.0058
Limbic	midage-old	0.0259
SMN	NA	-
Visual	NA	-

D. Discriminant Function Analysis and Importance of RSNs

Since metastability of different networks seem to be affected differently with age, we perform discriminant function analysis (DFA) to investigate which linear combination of the metastability of resting state networks can help discriminate between the three age groups significantly.

The metastability measures of 7 RSNs (predictors) were transformed into two-dimensional orthogonal space (defined by basis DF1 and DF2, referred as functions hereafter), which maximally discriminate between the age groups. Chi-square test of Wilk's lambda confirmed that mean ranks of the functions are significantly different across age groups (table 3). Loadings of each observed variable on the two functions is plotted in Fig. 5.

TABLE III. WILK'S LAMBDA

Test of Function	Wilk's Lambda	Chi-square	df	Sig.
1	.439	34.560	14	.002
2	.693	15.427	6	.017

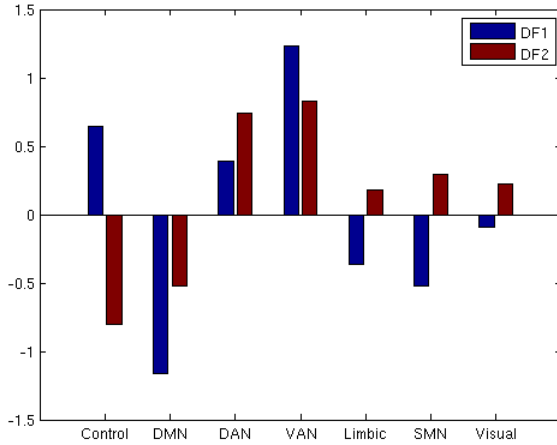


Fig. 5 Loadings of each variable on two functions (DF1 and DF2) identified by DFA. DF1 largely reflects the previously reported well-known dichotomy between salience, control (task positive) and DMN (task negative) networks while DF2 captures interesting pattern with strong positive effects of Ventral and Dorsal attention network together with strong negative effects of Control and Default Mode Network.

DF1 reflects the well known organization [2, 29] of “task-positive” (namely Control, Dorsal and Ventral attention systems) and “task negative” Default mode network. DF2 revealed interesting pattern of co-ordination between DMN and Control networks, which contrasts with attention networks. This pattern accounts for ~46% of the total variance in transformed space. Sensorimotor, visual and limbic systems negatively contribute to DF1 but positively contribute to DF2.

All groups were successfully discriminated on the two axis (Fig. 6). 72.9% of original grouped cases were correctly classified by the discriminant function. Leave-one out cross-validation resulted in 60.3% of accuracy. DF1 significantly ($H(2)=15.9$; $p=0.0004$) distinguished between young and middle-aged group ($p=0.0002$) as well as between young and elderly groups ($p=0.0032$) mostly on the basis of contrast between DMN and salience + control networks with younger subjects exhibiting lower metastability in DMN but higher metastability in salience, dorsal attention and control networks. DF2 significantly ($H(2)=16.69$; $p=0.0002$) discriminated between young and old groups ($p<0.0049$) as well as between middle-aged and old group ($p=0.0004$) with older subjects having higher metastability in dorsal and ventral attention networks but lower metastability in control and DMN. Fig. 7 captures rank-relationship between metastability of groups along the directions of DF1 and DF2.

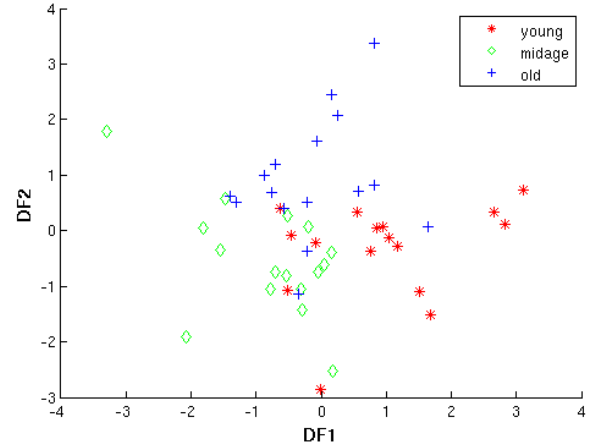


Fig. 6 DF1 against DF2. 72.9 % (and 60.3% after leave-one out cross-validation) of original data-points were successfully classified. Elderly adults have higher variance along positive DF2 axis while young and middle-aged adults show higher variance along positive and negative DF1 axis respectively.

The results of discriminant analysis suggest that there are two different combination of resting state network systems that are affected by age; each affected at the different point in lifespan. System ascribed to DF1 operates after the young age; during maturation and system described by DF2 operates at the old age, during ageing process.

IV. CONCLUSIONS & DISCUSSION

We studied effect of age on dynamic repertoire of the intrinsic activity of the brain. We evaluated metastability (i.e., ability of BOLD signals of cortical regions to co-ordinate and compete in time [30]) across three uniformly distributed age groups: young, middle-aged and old. We found significant differences in whole-brain metastability between old and middle-aged groups suggesting that older participants are likely to visit more distinct ‘states’ at rest than the middle-aged participants. Yeo *et al.*[31] has shown that functional

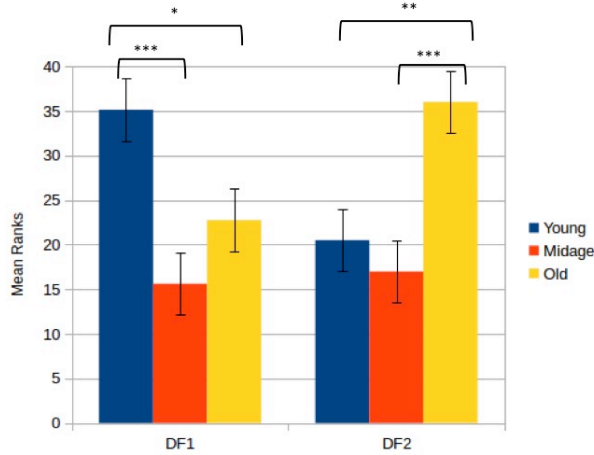


Fig. 7 Comparison of mean ranks on DF1 and DF2 obtained from post-hoc multiple comparisons on results of non-parametric one-way ANOVA. * $p < 0.05$, ** $p < 0.005$, *** $p < 0.0005$

entropy of the resting state networks increases with age, suggestive of more spatially widespread correlation pattern with age. Our results partially confirm this finding in temporal domain suggesting that increased entropy in static-FC of elderly adults might be a result of the increased variability in dynamic FC. In contrast to their results, such effect was not significant between young to middle-age.

Grady *et al.*[32] used partial least squares to assess age-effect on standard deviation of BOLD signals and confirmed wide-spread age-related patterns with some regions showing increased variability while others showing decrease with age. However, the study contained only young and elderly groups. Our results show that more robust patterns of variability exist between young to middle-aged as well as middle-aged to old.

To understand the metastable behavior across topologically distinct functional networks, we use community detection algorithm on mean-FC and compared metastability of detected communities across age groups. We found significant difference between middle-to-old age groups only in one community, which contained regions from control network and ventral attention network. However, on applying multivariate discriminant analysis across networks show that richer age-related differences exist due to combined effects of these networks, which remain largely undetectable by considering only static mean-FC for graph theoretic analysis. We also find that default mode network does not show significant age-effects in the independent univariate analysis. However, when taken together with other networks, it does contribute to the predictability of age.

Most interesting results were obtained from the discriminant analysis. We found two different patterns of change in metastability each of which significantly discriminate between maturation (young to middle-age) and ageing (middle-age to old) processes. Precisely, first pattern revealed higher metastability in control and attention systems

with lower metastability of default mode, limbic and sensorimotor systems in young subjects compared to other two groups. Second pattern showed reversed pattern in metastability of control, limbic and somatosensory (SMN and visual) networks. Precisely, old subjects have significantly higher metastability in attention networks, limbic and sensorimotor networks while significantly lower metastability in control and default mode regions than that of other two groups. This observation confirms claims of default-executive coupling hypothesis in old age [33], which precisely suggests reduced segregation between default mode and executive control network. We provide additional evidence that increased coupling between these two systems is most likely due to reduced metastability of control network in old age. Most striking difference between maturation to ageing process is therefore can be attributed precisely to the reversed role of control network in terms of its significantly lower metastability. We speculate that process of maturation might gradually converge to the process of ageing when the frontoparietal control network decouples from the attention networks and couples with the default mode regions due to reduction in metastability of this network.

V. LIMITATIONS & FUTURE WORK

The present study explored age-effect on the dynamic interactions between resting state functional networks. We found significant differences in whole-brain metastability of old adults than that of middle-aged. We also found changing role of functional network systems in terms of their metastability across age groups. One notable limitation is the cross-sectional nature of this study. Maturation and senescence are continuous processes affected by many other factors and cross sectional studies cannot account for the inter-individual variability that exist due to genetic, molecular, neural and environmental differences. Therefore test-retest validation of the results proposed here in a longitudinal cohort study with appropriate phenotyping is required. Moreover, changed metastability of BOLD signals does not necessarily reflect changed dynamics at neural level. Therefore, a computational approach is required to understand neural underpinnings of these age-related changes. How change in metastability is manifested at behavioral level is not yet well known. One might therefore consider similar analysis in task-based experimental setting and correlate metastability scores with the performance of elderly adults on various behavioral tests to understand whether the increased metastability of elderly adults is a beneficial or a detrimental process.

ACKNOWLEDGMENT

We thank Teradata Pvt. Ltd., Hyderabad for offering a financial support and travel grant if the manuscript is accepted for presentation.

REFERENCES

- [1] S. L. Bressler and J. S. Kelso, "Cortical coordination dynamics and cognition," *Trends in cognitive sciences*, vol. 5, pp. 26-36, 2001.
- [2] M. D. Fox and M. E. Raichle, "Spontaneous fluctuations in brain activity observed with functional magnetic resonance imaging," *Nature Reviews Neuroscience*, vol. 8, pp. 700-711, 2007.
- [3] R. F. Betzel, B. Mišić, Y. He, J. Rumschlag, X.-N. Zuo, and O. Sporns, "Functional brain modules reconfigure at multiple scales across the human lifespan," *arXiv preprint arXiv:1510.08045*, 2015.
- [4] C. Grady, S. Sarraf, C. Saverino, and K. Campbell, "Age differences in the functional interactions among the default, frontoparietal control, and dorsal attention networks," *Neurobiology of aging*, vol. 41, pp. 159-172, 2016.
- [5] D. Meunier, S. Achard, A. Morcom, and E. Bullmore, "Age-related changes in modular organization of human brain functional networks," *Neuroimage*, vol. 44, pp. 715-723, 2009.
- [6] J. Song, R. M. Birn, M. Boly, T. B. Meier, V. A. Nair, M. E. Meyerand, *et al.*, "Age-related reorganizational changes in modularity and functional connectivity of human brain networks," *Brain connectivity*, vol. 4, pp. 662-676, 2014.
- [7] U. Lindenberger, "Human cognitive aging: Corriger la fortune?," *Science*, vol. 346, pp. 572-578, 2014.
- [8] R. Cabeza, "Hemispheric asymmetry reduction in older adults: the HAROLD model," *Psychology and aging*, vol. 17, p. 85, 2002.
- [9] D. C. Park and P. Reuter-Lorenz, "The adaptive brain: aging and neurocognitive scaffolding," *Annual review of psychology*, vol. 60, p. 173, 2009.
- [10] P. A. Reuter-Lorenz and K. A. Cappell, "Neurocognitive aging and the compensation hypothesis," *Current directions in psychological science*, vol. 17, pp. 177-182, 2008.
- [11] P. A. Reuter-Lorenz and D. C. Park, "How does it STAC up? Revisiting the scaffolding theory of aging and cognition," *Neuropsychology review*, vol. 24, pp. 355-370, 2014.
- [12] E. C. Hansen, D. Battaglia, A. Spiegler, G. Deco, and V. K. Jirsa, "Functional connectivity dynamics: modeling the switching behavior of the resting state," *Neuroimage*, vol. 105, pp. 525-535, 2015.
- [13] J. Qin, S.-G. Chen, D. Hu, L.-L. Zeng, Y.-M. Fan, X.-P. Chen, *et al.*, "Predicting individual brain maturity using dynamic functional connectivity," *Frontiers in human neuroscience*, vol. 9, 2015.
- [14] P. J. Hellyer, G. Scott, M. Shanahan, D. J. Sharp, and R. Leech, "Cognitive flexibility through metastable neural dynamics is disrupted by damage to the structural connectome," *The Journal of Neuroscience*, vol. 35, pp. 9050-9063, 2015.
- [15] J. L. Baird and R. E. Van Emmerik, "Young and older adults use different strategies to perform a standing turning task," *Clinical Biomechanics*, vol. 24, pp. 826-832, 2009.
- [16] M. Schirner, S. Rothmeier, V. K. Jirsa, A. R. McIntosh, and P. Ritter, "An automated pipeline for constructing personalized virtual brains from multimodal neuroimaging data," *Neuroimage*, vol. 117, pp. 343-357, 2015.
- [17] R. S. Desikan, F. Ségonne, B. Fischl, B. T. Quinn, B. C. Dickerson, D. Blacker, *et al.*, "An automated labeling system for subdividing the human cerebral cortex on MRI scans into gyral based regions of interest," *Neuroimage*, vol. 31, pp. 968-980, 2006.
- [18] E. Glerean, J. Salmi, J. M. Lahnakoski, I. P. Jääskeläinen, and M. Sams, "Functional magnetic resonance imaging phase synchronization as a measure of dynamic functional connectivity," *Brain connectivity*, vol. 2, pp. 91-101, 2012.
- [19] J. Cabral, E. Hugues, O. Sporns, and G. Deco, "Role of local network oscillations in resting-state functional connectivity," *Neuroimage*, vol. 57, pp. 130-139, 2011.
- [20] G. Deco and M. L. Kringelbach, "Metastability and coherence: extending the communication through coherence hypothesis using a whole-brain computational perspective," *Trends in neurosciences*, vol. 39, pp. 125-135, 2016.
- [21] M. Rubinov and O. Sporns, "Complex network measures of brain connectivity: uses and interpretations," *Neuroimage*, vol. 52, pp. 1059-1069, 2010.
- [22] M. Rubinov and O. Sporns, "Weight-conserving characterization of complex functional brain networks," *Neuroimage*, vol. 56, pp. 2068-2079, 2011.
- [23] M. E. Newman, "Modularity and community structure in networks," *Proceedings of the national academy of sciences*, vol. 103, pp. 8577-8582, 2006.
- [24] B. T. Yeo, F. M. Krienen, J. Sepulcre, M. R. Sabuncu, D. Lashkari, M. Hollinshead, *et al.*, "The organization of the human cerebral cortex estimated by intrinsic functional connectivity," *Journal of neurophysiology*, vol. 106, pp. 1125-1165, 2011.
- [25] S. K. Kachigan, *Statistical analysis: An interdisciplinary introduction to univariate & multivariate methods*: Radius Press, 1986.
- [26] H. Scheffe, "A method for judging all contrasts in the analysis of variance," *Biometrika*, vol. 40, pp. 87-110, 1953.
- [27] B. G. Tabachnick, L. S. Fidell, and S. J. Osterlind, "Using multivariate statistics," 2001.
- [28] M. Fukushima, R. F. Betzel, Y. He, M. A. de Reus, M. P. Heuvel, X.-N. Zuo, *et al.*, "Individual variability and connectivity dynamics in modular organization of human cortical functional networks," *arXiv preprint arXiv:1511.06427*, 2015.
- [29] N. U. Dosenbach, D. A. Fair, F. M. Miezin, A. L. Cohen, K. K. Wenger, R. A. Dosenbach, *et al.*, "Distinct brain networks for adaptive and stable task control in humans," *Proceedings of the National Academy of Sciences*, vol. 104, pp. 11073-11078, 2007.
- [30] E. Tognoli and J. S. Kelso, "The metastable brain," *Neuron*, vol. 81, pp. 35-48, 2014.
- [31] Y. Yao, W. Lu, B. Xu, C. Li, C. Lin, D. Waxman, *et al.*, "The increase of the functional entropy of the human brain with age," *arXiv preprint arXiv:1406.1976*, 2014.
- [32] C. L. Grady and D. D. Garrett, "Understanding variability in the BOLD signal and why it matters for aging," *Brain imaging and behavior*, vol. 8, pp. 274-283, 2014.
- [33] G. R. Turner and R. N. Spreng, "Prefrontal engagement and reduced default network suppression co-occur and are dynamically coupled in older adults: the default-executive coupling hypothesis of aging," *Journal of cognitive neuroscience*, 2015.